

*Review paper*

## **Photoelectrochemical Cell and Its Applications in Optoelectronics**

*Di Wei\* and Gehan Amaratunga*

Centre of Advanced Photonics and Electronics, Department of Engineering, University of Cambridge, 9 JJ Thomson Av., Cambridge, UK.

\*Email: [dw344@cam.ac.uk](mailto:dw344@cam.ac.uk)

*Received:* 13 September 2007 / *Accepted:* 9 October 2007 / *Online published:* 20 October 2007

---

Electrochemistry is largely applied in synthesis, chemical analysis and energy storage and conversion aspects. Photoelectrochemistry as a branch of electrochemistry attracts extensive attention from scientists worldwide for its use to convert light energy into electricity with efficiencies competing with silicon based photovoltaics. This review will focus on the area of photoelectrochemical cell and its applications in optoelectronics, i.e. electrochemical photovoltaic cells, dye sensitized solar cells and light emitting cells. Most recent advances in above areas have been included.

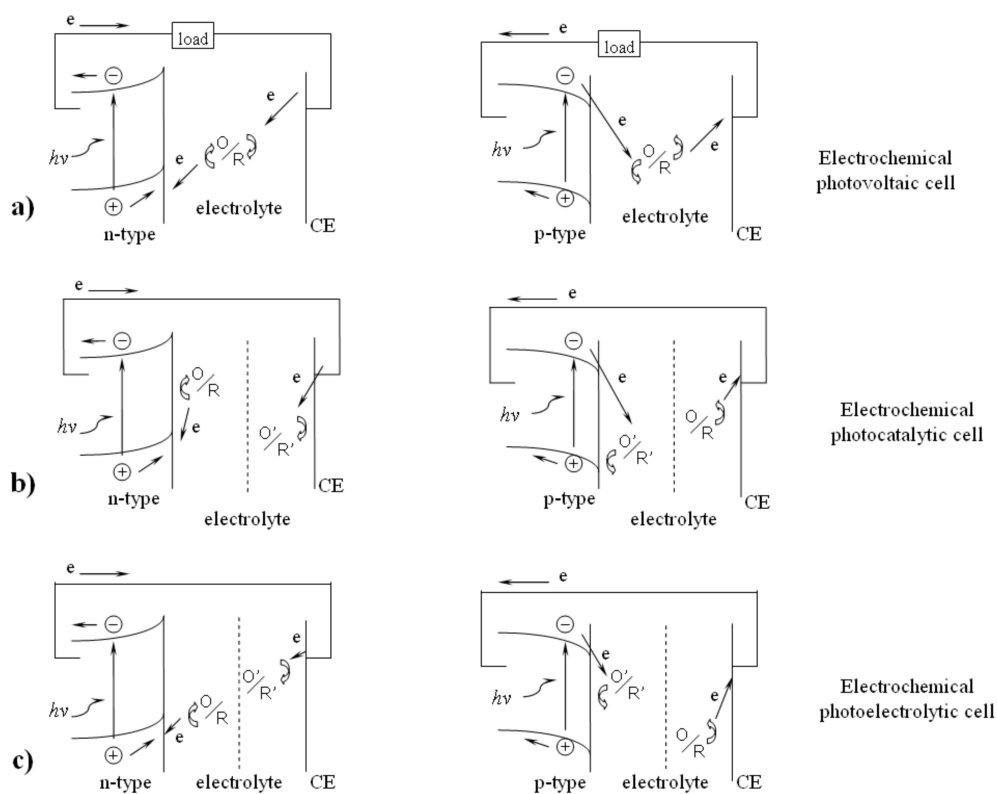
---

**Keywords:** photoelectrochemistry, photoelectrochemical photovoltaic cells, dye sensitized solar cells (DSSC), electrochemical light emitting cells.

### **1. INTRODUCTION**

A typical type of the photocurrent-generated device has a semiconductor in contact with an electrolyte, and this is often referred as photoelectrochemical cells. A photoelectrochemical cell consists of a photoactive semiconductor working electrode (either n- or p-type) and counter electrode made of either metal (e.g. Pt) or semiconductors. Both electrodes are immersed in the electrolyte containing suitable redox couples. In a metal-electrolyte junction, the potential drop occurs entirely on the solution site, whereas in a semiconductor-electrolyte junction, the potential drop occurs on the semiconductor site as well as the solution site. The charge on the semiconductor side is distributed deep in the interior of the semiconductor, creating a space charge region. If the junction of the semiconductor-electrolyte is illuminated with a light having energy greater than the bandgap of the semiconductor, photogenerated electrons/holes are separated in the space charge region. The photogenerated minority carriers arrive at the interface of the semiconductor-electrolyte.

Photogenerated majority carriers accumulate at the backside of the semiconductor. With the help of a connecting wire, photogenerated majority carriers are transported via a load to the counter electrode where these carriers electrochemically react with the redox electrolyte. A pioneering photoelectrochemical experiment was realized by obtaining photocurrent between two platinum electrodes immersed in the electrolyte containing metal halide salts [1]. It was later found that the photosensitivity can be extended to longer wavelengths by adding a dye to silver halide emulsions [2]. The interest in photoelectrochemistry of semiconductors led to the discovery of wet-type photoelectrochemical solar cells [3-5]. These studies showed electron transfer to be the prevalent mechanism for photoelectrochemical sensitization processes. Grätzel has then extended the concept to the dye sensitized solar cells (DSSC), which will be discussed further in the later part.



**Scheme 1** Different types of photoelectrochemical cells with the working electrode (WE) made of semiconductor (n- or p-type) and the counter electrode (CE).

Scheme 1 shows various types of the photoelectrochemical cells. When shining the light, oxidation reaction will happen on the surface of n-type semiconductors, whilst reduction reaction will happen on the surface of p-type semiconductors. In the electrochemical photovoltaic cell, which is based on a narrow bandgap semiconductor and a redox couple as shown in Scheme 1a, optical energy is converted into electrical energy without change of the free energy of the redox electrolyte ( $\Delta G=0$ ). The electrochemical reaction occurring at the counter electrode (CE) is opposite to the photoassisted

reaction occurring at the semiconductor working electrode. Thus, they are also called regenerative photoelectrochemical solar cells [6-9]. If the photogenerated energy is converted to chemical energy, the free energy of the electrolyte will have a change ( $\Delta G \neq 0$ ). Depending on the relative location of the potentials of the two redox couples (O/R and O'/R' in Scheme 1 b and c), the photosynthetic cells containing two redox couples, can be further classified as photocatalytic cell ( $\Delta G < 0$ , Scheme 1b) where light merely serves to accelerate the reaction rate and photoelectrolytic cell ( $\Delta G > 0$ , Scheme 1c) where the cell reaction is driven by light in the contra-thermodynamic direction. Comparing with electrochemical photovoltaic cells, anodic and cathodic compartments need to be separated to prevent the mixing of the two redox couples in these types of cells. Titanium dioxide ( $\text{TiO}_2$ ) has been favored semiconductor for such studies [10]. As early as 1971, photoelectrolysis of water was reported in an electrochemical cell with a  $\text{TiO}_2$  photoanode and a Pt cathode without an external source [11]. A novel microreactor for  $\text{TiO}_2$ -assisted photocatalysis in a microfluidic electrochemical cell was designed recently with  $\text{TiO}_2$  nanoparticles embedded in a gold electrode matrix [12]. The metal ions in aqueous solution can be determined by voltammetry after in situ photocatalytic digestion of interfering organic matter. This is very important for environmental analysis.

In this review, we will mainly focus on the development of regenerative electrochemical photovoltaic cells, dye sensitized solar cells and their reverse process, electrochemical light emitting cells. Absorption of light by the semiconductor or the sensitizer layer gives rise to a photocurrent and/or a photovoltage, which can be measured in the external circuit. Conversely, the passage of current through the interface of the working electrode with the electrolyte solution can lead to light emission.

## 2. ELECTROCHEMICAL PHOTOVOLTAIC CELLS

One of the most important aspects in using solar energy is its conversion from solar radiation into electric energy. Electrochemical photovoltaic cells have the following advantages comparing with the solid photovoltaics. 1) It is not sensitive to the defects in semiconductors. 2) The solid/liquid junction is easy to form and the production price will be much reduced. 3) It is possible to realize the direct energy transfer from photons to chemical energy. Unlike conventional solid state photovoltaic cells, the potential of the working electrode can be varied with respect to the reference electrode by means of an external voltage source connected between working and counter electrode.

### 2.1. Electrochemical photovoltaic cells without dyes

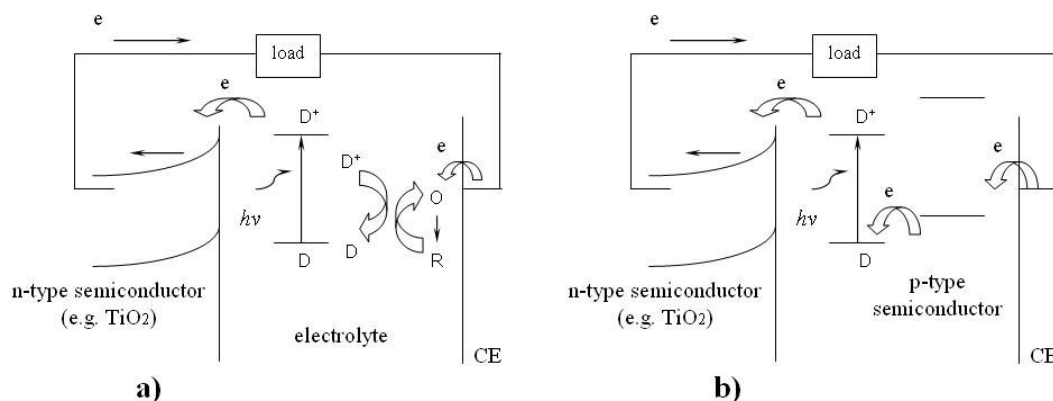
The most striking difference between a photoelectrochemical photovoltaic cell and the conventional Si based photovoltaics is that the former contains two interfaces at which charge transport has to switch from electronic to ionic and vice versa, as in batteries. In electrochemical photovoltaic cells without dyes, both the semiconductor electrode and the counter electrode are immersed in the redox electrolyte. The incident light excites the semiconductor electrode and the photogenerated electrons and holes are separated in the space charge region. Specific reactions occur

only at the semiconductor and the metal as shown in Scheme 1a. In these kinds of cell, charge balance due to oxidation and reduction processes is maintained. However, the wet-type photoelectrochemical cells suffer from instability of semiconductor in aqueous media. Unsensitized photoelectrochemical photovoltaic cells can not replace the silicon based photovoltaics unless some photoelectrochemically stable semiconductor materials possessing band gap approximately 1.4 eV can be found [6-9].

## 2.2. Dye sensitized solar cells (DSSC)

A novel solar cell based on a dye sensitized porous nanocrystalline  $\text{TiO}_2$  photoanode with attractive performance has been reported by Grätzel et al. [13-16]. Interest in porous semiconductor matrices permeated by an electrolyte solution containing dye and redox couples has been stimulated by their reports. The conversion efficiency of the dye sensitized solar cells (DSSC) has been currently improved to above 11% [15;17] since the first DSSC was reported with efficiency of 7.1% [16]. Even though silicon champion cells have attained 24%, the maximum conversion efficiency is approximately 30% for both devices [18]. Large-size DSSC has been prepared on silver grid embedded fluorine-doped tin oxide (FTO) glass substrate by screen printing method [19]. Under the standard test condition, energy conversion efficiency of active area was achieved to 5.52% in 5 cm $\times$ 5 cm device, which is comparable to 6.16% of small-size cell prepared at similar condition.

In DSSC, the initial photoexcitation does not occur in the semiconductor working electrode as the electrochemical photovoltaic cells in Scheme 1a, but occurs in the light absorbing dye as shown in Scheme 2. Subsequent injection of an electron from the photo-excited dye into the conduction band of semiconductors results in the flow of current in the external circuit. Sustained conversion of light energy is facilitated by regeneration of the reduced dye (D in Scheme 2) either via a reversible redox couple (O/R), which is usually  $\text{I}_3^-/\text{I}^-$  (Scheme 2a) or via the electron donation from a p-type semiconductor (Scheme 2b).



**Scheme 2** Operation mechanism of the dye sensitized electrochemical solar cell (DSSC). D: Dye, O: Oxidant (e.g,  $\text{I}_3^-$ ), R: Reductant (e.g.  $\text{I}^-$ ). a) Wet-type DSSC with redox couple in the liquid electrolyte b) Solid state DSSC with a p-type semiconductor to replace the electrolyte containing the redox couple.

Scheme 2a shows the mechanism of a traditional wet-type DSSC containing redox couples in electrolyte. The photoanode, made of a mesoporous dye-sensitized n-type semiconductor, receives

electrons from the photo-excited dye (D) which is thereby oxidized to  $D^+$ . The neutral dye (D) can be regenerated by the oxidation reaction ( $R \rightarrow O$ ) of the redox species dissolved in the electrolyte. The mediator R will then be regenerated by reduction at the cathode ( $O \rightarrow R$ ) by the electrons circulated through the external circuit [17].

The need for DSSC to absorb far more of the incident light was the driving force for the development of mesoscopic semiconductor materials with an enormous internal surface area. High photon to electron conversion efficiencies were reported based on the dye sensitized mesoporous  $TiO_2$  solar cells [20]. The major breakthrough in DSSC was the use of a high surface area nanoporous  $TiO_2$  layer. A single monolayer of the dye on the semiconductor surface was sufficient to absorb essentially all the incident light in a reasonable thickness (several  $\mu m$ ) of the semiconductor film.  $TiO_2$  became the semiconductor of choice with advantage properties of cheap, abundant, and non-toxic [21].

The standard dye at time was tris(2,2'-bipyridyl-4,4'-carboxylate)ruthium (II) ( $N_3$  dye). The function of the carboxylate group in the dye is to attach the semiconductor oxide substrate by chemisorption [21;22]. The dye must carry attachment groups such as carboxylate or phosphonate to firmly graft itself to the  $TiO_2$  surface. The attachment group of the dye ensures that it spontaneously assembles as a molecular layer upon exposing the oxide film to a dye solution. It will make a high probability that, once a photon is absorbed, the excited state of the dye molecule will relax by electron injection to the semiconductor conduction band. Discovered in 1993, the photovoltaic performance of  $N_3$  dye has been irreplaceable by other dye complexes [23]. Only recently a credible challenger has been identified with tri(cyanato-2,2',2''-terpyridyl-4,4',4''-tricarboxylate) Ru (II) (black dye) [15]. The response of the black dye extends 100 nm further into the IR than that of the  $N_3$  dye [24].

Because of the encapsulation problem posed by the use of the liquid in the conventional wet-type DSSC, much work is being done to make an all solid state DSSC [20;25]. The use of solvent free electrolytes in the DSSC is supposed to offer very stable performance for the device. To construct a full solid-state DSSC, a solid p-type conductor should be chosen to replace the liquid electrolyte. The redox levels of the dye and p-type materials have to be adapted carefully as Scheme 2b shows. It results in an electron in the conduction band of n-type semiconductors (e.g.  $TiO_2$ ) and a hole localized on the p-type conductor. Hole transporting amorphous materials have been used in nanocrystalline  $TiO_2$  based DSSC to transport hole carriers from the dye cation radical to the counter electrode instead of using the  $I_3^-/I^-$  redox species [20;26].

Early work focused on the replacement of  $I_3^-/I^-$  liquid electrolyte with CuI. CuI as a p-type conductor, can be prepared by precipitation from an acetonitrile solution at room temperature and it is also a solid state ionic conductor. Cells made this way gave solar efficiencies of several percent, but their stability is relatively poor, because of the liability of CuI to air and light [25]. Besides CuI, CuSCN has also been tried [27;28]. Organic hole transporting materials will offer flexibility and easier processing. Bach et al. used a hole conducting amorphous organic solid deposited by spin coating [20]. However, deposition in nanoporous materials can not be easily achieved by traditional methods such as evaporation or spin coating. Electrochemical deposition of organic semiconductors on high surface area electrodes for solar cells has also been described [29]. A thin layer of organic semiconductors can be electrochemically deposited on a nanoporous  $TiO_2$  electrode.

One of the first solid state dye sensitized heterojunctions between  $\text{TiO}_2$  and a semiconducting polymer was reported by Murakoshi and coworkers [30;31]. The prototype of this kind of solid state DSSC is shown in Fig. 1.

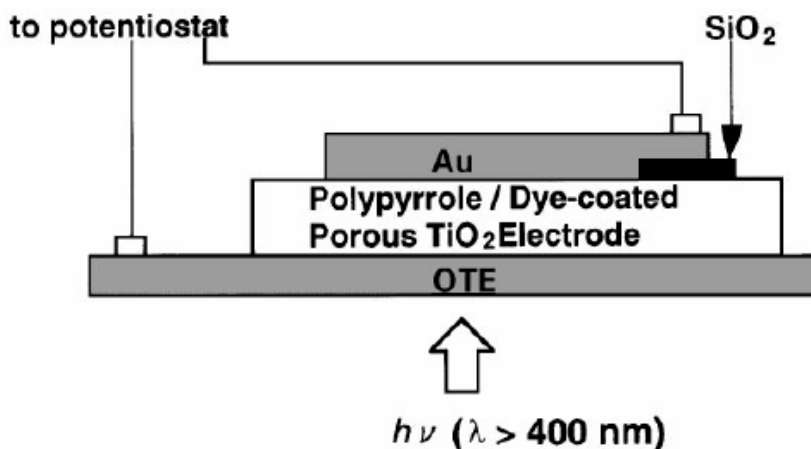


**Figure 1.** The prototype solid state DSSC [30]. OTE: Optical transparent electrode. Reproduced by kind permission from Elsevier Science Ltd.

Pyrrrole was photoelectrochemically polymerized on porous nanocrystalline  $\text{TiO}_2$  electrode, which was sensitized by  $\text{N}_3$  dye and a newly synthesized dye individually. Polypyrrole successfully worked as a hole transport layer connecting dye molecules anchored on  $\text{TiO}_2$  to the counter electrode. Conducting polyaniline has also been used in solid state solar cells sensitized with methylene blue [32]. This solid state DSSC was fabricated using conducting polyaniline coated electrodes sandwiched with a solid polymer electrolyte, viz. poly(vinyl alcohol) with phosphoric acid. It exhibits good photoresponse to visible light. The presence of illumination enhances the electrochemical reaction (doping of polyaniline by migration of anions). The observed I-V characteristics are the superposition of the Ohmic charge transport and the electrochemical reaction. Recently, a low bandgap polymer consisting of alternating thiophene and benzothiadiazole derivatives was used in the bulk heterjunction DSSC. This solid state DSSC exhibited a high power conversion efficiency of 3.1%, which is the highest power conversion efficiency value with organic hole-transport materials in DSSC to date [33].

Construction of quasi-solid-state DSSC has also been explored. Quasi-solid-state DSSCs based on the stable polymer grafted nanoparticle composite electrolyte [34], cyanoacrylate electrolyte matrix [35], and a novel efficient absorbent for liquid electrolyte based on poly(acrylic acid)-poly(ethylene glycol) hybrid [36] were fabricated. The polymer gels in above cases function as ionic conductors. The melting salt, in another name, room temperature ionic liquids are also known as good ionic conductors [37;38]. Solid state DSSCs based on ionic liquids were reported to enhance the conversion efficiency of DSSCs [39]. DSSCs using imidazolium type ionic liquid crystal systems as effective electrolytes were reported [40]. Use of ionic liquid oligomers, which were prepared by incorporating imidazole ionic liquid with polyethylene oxide oligomers, as electrolyte for DSSC was investigated [41]. It shows that the increase of the polyethylene oxide molecular weight in the ionic liquid oligomers results in faster dye regeneration and lower charge transfer resistance of  $\text{I}_3^-$  reduction leading to the

improvement of DSSC performance. However, the main limiting factors in the DSSC based on ionic liquids comparing with the conventional wet-type DSSC are the higher recombination and lower injection of charge. At low temperatures, the higher diffusion resistance in the ionic liquid may also be the main limiting factor through its effect to the fill factor [42]. Plastic and solid state DSSCs incorporating single walled carbon nanotubes (SWNTs) and imidazorium iodide derivative have been fabricated [43]. The introduction of carbon nanotubes will improve the solar cell performance through reduction of the series resistance. TiO<sub>2</sub> coated carbon nanotubes (CNTs) were recently used in DSSCs. Compared with a conventional TiO<sub>2</sub> cell, the TiO<sub>2</sub>-CNT (0.1 wt%) cell gives an increase to short circuit current density ( $J_{SC}$ ), which results in ~50% increase in conversion efficiency from 3.32% to 4.97% [44]. It is supposed that the enhancement of  $J_{SC}$  is due to improvement in interconnectivity between the TiO<sub>2</sub> particles and the TiO<sub>2</sub>-CNTs in the porous TiO<sub>2</sub> film. When employing SWNTs as conducting scaffolds in a TiO<sub>2</sub> based DSSC, the photoconversion efficiency can be boosted by a factor of 2 [45]. In absence of SWNT network, a maximum IPCE of 7.36% (350 nm) at 0 V (vs. SCE) was observed. The IPCE was enhanced significantly to 16% when the SWNT scaffolds support the TiO<sub>2</sub> particles. TiO<sub>2</sub> nanoparticles were dispersed on SWNT films to improve photoinduced charge separation and transport of carriers to the collecting electrode surface.

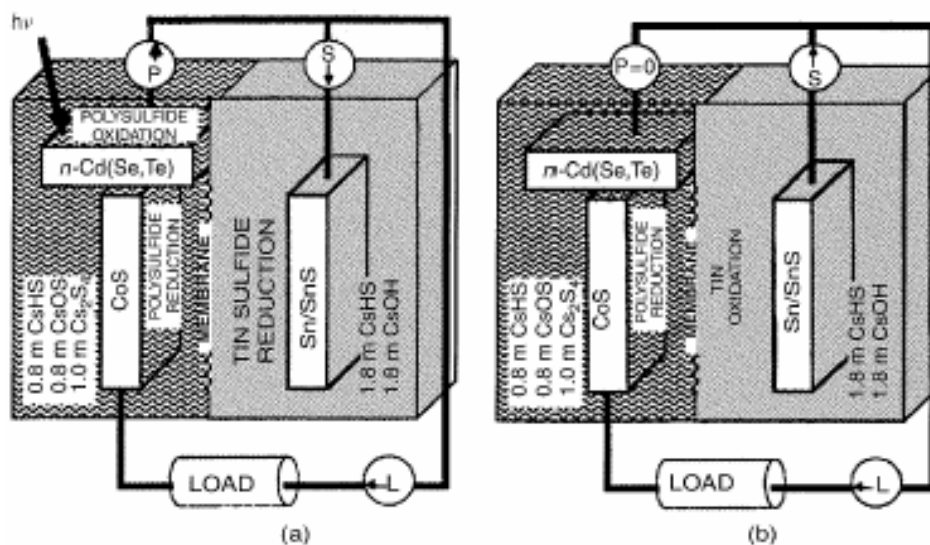
A strong increase in energy conversion efficiency could also be observed when tertiarybutylpyridine was introduced into the matrix of the organic hole conductor [46] with similar effects for classic DSSC with electrolyte/TiO<sub>2</sub> junctions [23]. The increase in  $V_{oc}$  may be due to either a charging of surface states or a shift of the conduction band edge [47]. Lithium ion interactions into TiO<sub>2</sub>-B nanowires [48], nanocrystalline rutile TiO<sub>2</sub> particles [49] and a class of perovskite based lithium ion conductors [50] have been reported. Photovoltages of nanoporous TiO<sub>2</sub> based DSSC was found to be improved by up 200 mV with a negligible decrease in photocurrent by treating TiO<sub>2</sub> electrodes with intercalation of Li<sup>+</sup> [51]. The enhancement of photovoltage is explained in terms of the formation of a dipole layer due to adsorption of Li<sup>+</sup> on the TiO<sub>2</sub> surface generated by the reaction of intercalated Li atoms with moisture in air. Addition of lithium salt Li[(CF<sub>3</sub>SO<sub>2</sub>)<sub>2</sub>N] to the spin coating solution of the hole conductor also resulted in a strong performance increase in the final device. The underlying mechanism remained unidentified although charge screening due to partial ionic mobility inside the hole conductor matrix and/or the effect of the present lithium ions on the flat band potential of TiO<sub>2</sub> were postulated as possible mechanisms [52].

Other n-type semiconducting electrodes besides TiO<sub>2</sub> have been probed for DSSC. The best studied of the alternative materials to TiO<sub>2</sub> is ZnO [53-55]. ZnO has similar band gap (3.2 eV) and band edge position to TiO<sub>2</sub> [56] with similar or smaller crystallite sizes than for typical TiO<sub>2</sub>. The fabrication of DSSC with a branched structure of ZnO nanowires was recently reported [57]. The striking optical properties of nanoporous silicon obtained by photoanodic etching [58] extended the materials research scope of photoelectrochemistry to other porous crystalline semiconductors [59]. At present, there is a considerable effort being devoted to DSSC with nanoporous photoanodes [16;60]. Nanoporous semiconductor electrodes were further investigated within the scope of quantum dots. Photoelectrochemical activity has been shown when the quantum dots such as CdS and PbS are attached to a metal electrode in a sub-monolayer array [61-65]. An ordered or disordered monolayer/sub-monolayer of nanometer-sized semiconductor particles (e.g. PbS quantum dots) can be

attached to a conducting substrate either by directly or via a self-assembled organic monolayer [66;67]. Photoelectrochemical study of organic-inorganic hybrid thin films via electrostatic layer by layer assembly was reported [68]. Although the self-assembly approach is useful to obtain an ordered array of quantum dots in the film, it does not provide robust coverage on the electrode surface. The research on size quantization in colloid systems develops new fields in photoelectrochemistry. In addition to the various methods to produce semiconductor quantum dots and nanocrystals with colloidal solution chemistry [69-72], semiconductor nanocrystals, quantum wires, quantum dots as well as thick films of CdS, CdSe and PbS can be made by electrochemical deposition methods [73-76]. This provides a new way to produce nanoporous semiconductor electrodes for DSSCs.

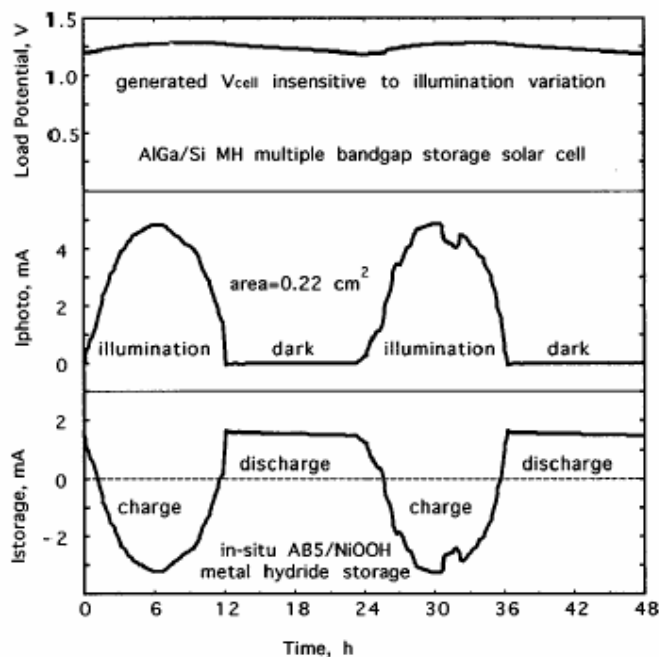
### 2.3. Storage of electrochemical energy

It is also possible to make a rechargeable battery with in situ storage capability by using the photoelectrochemical cells [77-79].



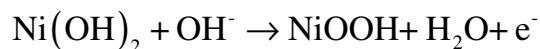
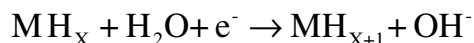
**Figure 2.** Schematic of a photoelectrochemical solar cell combining both solar conversion and storage capabilities. (a) under illumination, (b) in the dark. [77] Reproduced by kind permission from Nature.

Fig. 2 presents the configuration of a photoelectrochemical cell combining in situ electrochemical storage and solar conversion capabilities and it provides continuous output insensitive to daily variations in illumination. A high solar to electric conversion efficiency cell configuration of this type was demonstrated in 1987 and used a Cd (Se, Te)/S<sub>x</sub> conversion half cell and a Sn/SnS storage system, resulting in a solar cell with a continuous output [77]. Under illumination, as shown in Fig. 2a, the photocurrent drives an external load. Simultaneously, a portion of the photocurrent is used in the direct electrochemical reduction of metal cations ( $\text{Sn}^{2+} \rightarrow \text{Sn}$ ) in the device storage half cell. In darkness or below a certain level of light, the storage compartment spontaneously delivers power by metal oxidation ( $\text{Sn} \rightarrow \text{Sn}^{2+}$ ) as seen in Fig. 2b. This genius idea was further developed and the DSSC performance was improved significantly by using multi-band gap cells with storage.

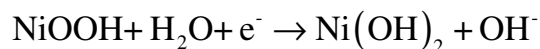
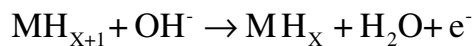


**Figure 3.** Two days conversion and storage characteristics of the AlGaAs/Si/MH/NiOOH multiple bandgap photoelectrochemical solar cell using a graded diffuse filter varied AM0 illumination. [78] Reproduced by kind permission from American Institute of Physics.

Because of the low fraction of short wavelength solar spectrum, wide band gap solar cells generate a high photovoltage but have low photocurrent. Smaller bandgap cells can use a large fraction of the incident photons, but generate lower photovoltage. Multiple band gap devices can overcome these limitations. In stacked multijunction systems, the topmost cell absorbs (and converts) energetic photons, but it is transparent to lower energy photons. Subsequent layers absorb lower energy photons. Conversion efficiency can be enhanced. A high solar conversion and storage efficiencies have been attained with a system that combines efficient multiple bandgap semiconductors, with a simultaneous high capacity electrochemical storage [78;80]. It provides a nearly constant energy output in illumination or dark conditions as shown in Fig. 3. The cell combines bipolar AlGaAs and Si and metal hydride(MH)/NiOOH storage. AlGaAs and Si are critical to minimize dark current, provide Ohmic contact without absorption loss and maximize cell efficiency. Under illumination, a fraction of the photo-generated electrons drives a load, while the remainder charges the storage redox couple via electrochemical processes such as metal hybrid  $MH_x$  reduction. The reduction will induce the increase in concentration of  $[OH^-]$  that drives the oxidation of  $Ni(OH)_2$  to NiOOH.



In darkness, the potential falls below  $E_{\text{redox}}$ , the storage redox couple spontaneously discharges. The electrochemical storage process then utilizes the metal hybrid  $\text{MH}_{\text{X}+1}$  anode oxidation and the  $\text{NiOOH}$  cathode reduction as shown by the equations below.



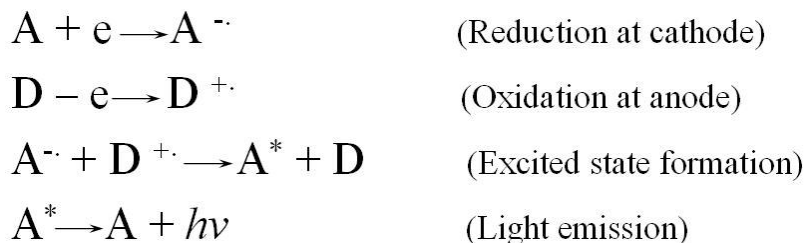
This dark discharge will be directed through the load. As shown in Fig. 3, the cell generates a light variation insensitive potential of 1.2 – 1.3 V with total solar-electric energy conversion efficiency over 18%.

### 3. ELECTROCHEMICAL LIGHT EMITTING CELLS

The reverse process of electrochemical photovoltaic cells is the electrochemical light emitting cells, which consists part of optoelectronics.

#### 3.1. Electrochemiluminescence

Electrochemiluminescence (ECL) is the process where species generated at electrodes undergoes electron transfer reactions to form excited states that emit light. ECL is initiated and controlled by changing an electrode potential. Classic ECL involves the formation of an excited state as a result of an energetic electron transfer between electrochemically generated species (often radical ions) at the surface of an electrode. ECL reactions are localized spatially, temporally and controllable. A typical ECL system would involve a solution containing ECL precursors with supporting electrolyte in an electrochemical cell with either a single working electrode using an alternative potential, or more commonly two separated electrodes in close proximity to each other by holding one electrode at a reductive potential and the other at an oxidative potential [81].



**Scheme 3.** General mechanism of electrochemiluminescence.

A general ECL mechanism with two-electrode set up is shown in Scheme 3. Species A accepts one electron from the cathode to form  $\text{A}^{\cdot -}$ , and species D loses one electron at the anode to form  $\text{D}^{\cdot +}$ . When  $\text{A}^{\cdot -}$  and  $\text{D}^{\cdot +}$  diffuse away from the electrodes and come together,  $\text{A}^{\cdot -}$  transfers one electron to  $\text{D}^{\cdot +}$

to produce a neutral species D and the excited state A\*. A\* immediately emits light and returns to the ground state A. A and D could be the same species such as a polycyclic aromatic hydrocarbon [82;83].

ECL is traditionally a very powerful analytic technique and has been widely used in many different areas [84-91]. In this review, use of electrochemiluminescence in light emitting cells will be focused.

### 3.2. Polymer electrochemical light emitting cells

Device configurations for light emission from electroactive polymers and organic molecules have been described by many papers [92-99]. In these kinds of electrochemical light emitting cells (LEC), a *p-n* junction diode is created in situ through simultaneous *p*-type and *n*-type electrochemical doping on opposite sides of a thin film of conjugated polymer that contains added electrolyte to provide the necessary counterions for doping. Besides using liquid electrolytes, polymer electrolytes were also applied by complexation of an ionically conducting polymer, such as polyethylene oxide (PEO) with salts. In contrast to the traditional light emitting diodes (LEDs) where the active layer does not contain any ionic species, a polymer LEC is based on a mixed ionic/electronic conductor consisting of a solid state polymer electrolyte and a luminescent polymer. The polymer electrolyte contributes and transports free ions. Cyclic voltammetry studies have been carried out on polymer electrochemical LEC using poly(2-methoxy-5-(2'-ethyl-hexyloxy)-1,4-phenylene vinylene), MEH-PPV, as the active luminescent polymer [92]. The onset of electronic current in the LEC is coincident with the onset of electrochemical doping and the formation of a *p-n* junction. Blue, green, and orange emission have also been obtained with turn-on voltages close to the band gap of the emissive material [93].

Polymer electrochemical LECs possess many desirable device characteristics suitable for potential display applications. The operating mechanism of this type of LEC involves in situ electrochemical doping and the formation of a light emitting *p-n* junctions, which have been confirmed by the demonstrations and direct imaging of extremely large planar LECs with an interelectrode spacing up to 1.1 to 1.5 mm as shown in Fig. 4 [100-102]. When a large enough voltage is applied, electrons and holes are injected to the cathode and anode individually and subsequently compensated by the insertion of free cations and anions between the polymer chains in the vicinity of the electrodes. As a result, the luminescent polymer is electrochemically doped to *p* type on the anode side and *n* type on the cathode side. With time the *p* and *n* doped regions expand towards the centre of the device until they make contact to form a *p-n* junction. The position of the light emitting junctions can be determined by direct optical probing of the doping progress and simultaneous recording of the current-time behavior [103]. The initial formation of a *p-n* junction triggers a sharp increase in both doping level and current flow. This is accompanied by the onset of electroluminescence in the vicinity of the junction, caused by the radiative recombination of the injected electrons and holes.

High resolution fluorescence imaging of the LEC structures reveals two fundamental problems for a conventional LEC. First, the luminescent polymer suffers significant photoluminescence quenching due to heavy doping throughout the polymer film. Second, the electroluminescence emission zone in an LEC is limited to less than 10% of the entire inter-electrode spacing. Both factors severely limit the ultimate electroluminescence efficiency of an LEC. The problem of heavy

photoluminescence quenching associated with a p-n junction has been recently overcome by intentionally relaxing a fully formed p-n junction into a p-i-n junction [104;105]. A frozen p-n junction in an LEC can relax into a p-i-n junction when heated briefly to above glass transition temperature of the polymer electrolyte used [106]. This results in a less doped quasi 'intrinsic' emission zone with much reduced photoluminescence quenching. A dramatic improvement in electroluminescence efficiency has been due to the formation of this 'intrinsic' emission zone when doping relaxes preferentially in the junction region [107;108]. In addition, a 20-fold increase in effective emitting area has been achieved by introducing floating metallic strips or particles between the electrodes, which leads to the formation of multiple light emitting p-n junctions [109]. These two approaches promise revolutionary LECs with the highest electroluminescence efficiency of all polymer light emitting devices. Recently long-life time polymer LECs have been made by mixing luminescent polymer blended with a dilute concentration of ionic liquids [110].

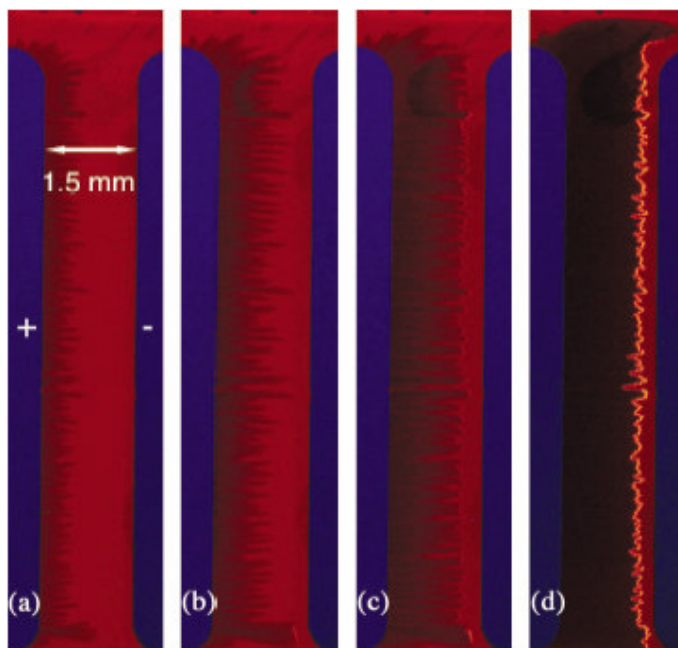


**Figure 4.** Colored photographs of a working 1.5 mm MEH-PPV polymer LEC under 365 nm UV illumination. The device was tested at 310 K under a voltage bias of 140 V. The electrode to the left is positively biased anode, denoted as '+' relative to the electrode to the right cathode, denoted as '-'. The photographs were taken at different time after the application of the voltage bias: (a) 8 min; (b) 13 min; (c) 18 min; (d) 43 min. [100] Reproduced by kind permission from American Institute of Physics.

### 3.5. Others

Use of organic conjugated materials has also been exploited for the realization of electrochemically driven electrochromics [111]. Recently, a photoelectrochromic cell is fabricated with a silver counter electrode and a transparent working electrode coated with a Ag-TiO<sub>2</sub> nanocomposite, which exhibits multicolour photochromism in an electrolyte containing silver ions [112]. The photoelectrochromic

cell operates in drawing mode (short circuit) and display mode (open circuit), and is initialized by polarization. The concepts of drawing and display modes are important to develop practical display devices based on the multicolour photochromism.

#### 4. CONCLUSIONS

Effective photovoltaics, light emitting and photoelectrochromic cells can be realized by means of electrochemical methods. Solid state DSSC and electrochemical light emitting cells will have a promising future for the development of efficient and flexible optoelectronics. Although a long way to compete with the silicon based ones in markets, the subject of photoelectrochemistry is the fundamental and will be a vivid subject to realize the device design and technology transfer.

#### Reference

1. A. E. Becquerel, *C. R. Acad. Sci.*, 9 (1839) 145.
2. W. West, *Proc. VogelCent. Symp. Photogr. Sci. Eng.*, 18 (1974) 35.
3. H. Gerischer and H. Tributsch, *Ber. Bunsenges. Phys. Chem.*, 72 (1968) 437.
4. K. Hauffe, H. J. Danzmann, H. Pusch, J. Range, and H. Volz, *J. Electrochem. Soc.*, 117 (1970) 993.
5. V. A. Myamlin and Y. V. Pleskov, *Electrochemistry of Semiconductors*, Plenum Press, New York, 1967.
6. A. B. Ellis, S. W. Kaiser, and M. S. Wrighton, *J. Am. Chem. Soc.*, 98 (1976) 1635.
7. A. B. Ellis, J. M. Bolts, and M. S. Wrighton, *J. Electrochem. Soc.*, 124 (1977) 1603.
8. G. Hodes, J. Manassen, and D. Cahen, *Nature*, 261 (1976) 403.
9. B. Miller and A. Heller, *Nature*, 262 (1976) 680.
10. A. Fujishima and K. Honda, *Nature*, 238 (1972) 37.
11. A. Fujishima and K. Honda, *Bull. Chem. Soc. Jpn.*, 44 (1971) 1148.
12. D. Daniel and I. G. R. Gutz, *Electrochem. Commun.*, 9 (2007) 522.
13. M. Grätzel, *Nature*, 421 (2003) 586.
14. M. Grätzel, *J. Photochem. & Photobio. A*, 164 (2004) 3.
15. A. Hagfeldt and M. Grätzel, *Acc. Chem. Res.*, 33 (2000) 269.
16. B. O'Regan and M. Grätzel, *Nature*, 353 (1991) 737.
17. M. Grätzel, *Nature*, 414 (2001) 338.
18. M. Grätzel, *Phil. Trans. R. Soc. A*, 365 (2007) 993.
19. W. J. Lee, E. Ramasamy, D. Y. Lee, and J. S. Song, *Sol. Energy Mater. Sol. Cells*, 91 (2007) 1676.
20. U. Bach, D. Lupo, P. Comte, J. E. Moser, F. Weissortel, J. Salbeck, H. Spreitzer, and M. Grätzel, *Nature*, 395 (1998) 583.
21. N. Vlachopoulos, P. Liska, J. Augustynski, and M. Grätzel, *J. Am. Chem. Soc.*, 110 (1988) 1216.
22. J. De Silvestro, M. Grätzel, L. Kavan, J. Moser, and J. Augustynski, *J. Am. Chem. Soc.*, 107 (1985) 2988.
23. M. K. Nazeeruddin, A. Kay, I. Rodicio, R. Humphry-Baker, E. Muller, P. Liska, N. Vlachopoulos, and M. Grätzel, *J. Am. Chem. Soc.*, 115 (1993) 6382.

24. M. K. Nazeeruddin, P. Pechy, T. Renouard, S. M. Zakeeruddin, R. H. Baker, P. Comte, P. Liska, L. Cevey, E. Costa, V. Shklover, L. Spiccia, G. B. Deacon, C. A. Bignozzi, and M. Grätzel, *J. Am. Chem. Soc.*, 123 (2001) 1613.
25. K. Tennakone, G. R. R. A. Kumara, I. R. M. Kottegoda, K. G. U. Wijanthana, and P. S. Perera, *J. Phys. D:Appl. Phys.*, 31 (1998) 1492.
26. J. Hagen, W. Schaffrath, P. Otschik, R. Fink, A. Bacher, H. W. Schmidt, and D. Haarer, *Synth. Met.*, 89 (1997) 215.
27. B. O'Regan and D. T. Schwartz, *Chem. Mater.*, 7 (1995) 1349.
28. B. O'Regan, D. T. Schwartz, S. M. Zakeeruddin, and M. Grätzel, *Adv. Mater.*, 12 (2000) 1263.
29. A. Zaban and Y. Diamant, *J. Phys. Chem. B.*, 104 (2000) 10043.
30. K. Murakoshi, R. Kogure, Y. Wada, and S. Yanagida, *Sol. Energy Mater. Sol. Cells*, 55 (1998) 113.
31. K. Murakoshi, R. Kogure, and S. Yanagida, *Chem. Lett.*, 5 (1997) 471.
32. P. R. Somani and S. Radhakrishnan, *J. Solid State Electrochem.*, 7 (2003) 166.
33. W. S. Shin, S. C. Kim, S. J. Lee, H. S. Jeon, M. K. Kim, B. V. K. Naidu, S. H. Jin, J. K. Lee, J. W. Lee, and Y. S. Gal, *J. Poly. Sci. ,A. ,Poly. Chem.*, 45 (2007) 1394.
34. X. Zhang, H. Yang, H. M. Xiong, F. Y. Li, and Y. Y. Xia, *J. Power Sources*, 160 (2006) 1451.
35. S. L. Lu, R. Koeppel, S. Gunes, and N. S. Sariciftci, *Sol. Energ. Mater. Sol. C.*, 91 (2007) 1081.
36. Z. Lan, J. Wu, J. Lin, and M. Huang, *J. Power Sources*, 164 (2007) 921.
37. M. Galinski, A. Lewandowski, and I. Stepniak, *Electrochim. Acta*, 51 (2006) 5567.
38. K. E. Johnson, *Interface*, 16 (2007) 38.
39. P. Wang, S. M. Zakeeruddin, J. E. Moser, and M. Grätzel, *J. Phys. Chem. B.*, 107 (2003) 13280.
40. N. Yamanaka, R. Kawano, W. Kubo, N. Masaki, T. Kitamura, Y. Wada, M. Watanabe, and S. Yanagida, *J. Phys. Chem. B*, 111 (2007) 4763.
41. M. Wang, X. Xiao, X. Zhou, X. Li, and Y. Lin, *Sol. Energ. Mater. Sol. C.*, 91 (2007) 785.
42. F. Fabregat-Santiago, J. Bisquert, E. Palomares, L. Otero, D. Kuang, S. M. Zakeeruddin, and M. Grätzel, *J. Phys. Chem. C.*, 111 (2007) 6550.
43. N. Ikeda and T. Miyasaka, *Chem. Lett.*, 36 (2007) 466.
44. T. Y. Lee, P. S. Alegaonkar, and J. B. Yoo, *Thin Solid Films*, 515 (2007) 5131.
45. A. Kongkanand, R. M. Dominguez, and P. V. Kamat, *Nano Lett.*, 7 (2007) 676.
46. U. Bach, J. Kruger, and M. Grätzel. SPIE Proceedings San Diego. 2000.  
Ref Type: Conference Proceeding
47. S. Y. Huang, G. Schlichthorl, A. J. Notzik, M. Grätzel, and A. J. Frank, *J. Phys. Chem. B.*, 101 (1997) 2576.
48. A. R. Armstrong, G. Armstrong, J. Canales, R. Garcia, and P. G. Bruce, *Adv. Mater.*, 17 (2005) 862.
49. M. A. Reddy, M. S. Kishore, V. Pralong, V. Caignaert, U. V. Varadaraju, and B. Raveau, *Electrochem. Commun.*, 8 (2006) 1299.
50. P. M. Woodward, *Nature Materials*, 6 (2007) 549.
51. Y. Hairima, K. Kawabuchi, S. Kajihara, A. Ishii, Y. Ooyama, and K. Takeda, *Appl. Phys. Lett.*, 90 (2007) 103517.
52. B. Enright, G. Redmond, and D. Fitzmaurice, *J. Phys. Chem.*, 97 (1993) 1426.
53. P. Hoyer and H. Weller, *J. Phys. Chem.*, 99 (1995) 14096.
54. H. Rensmo, K. Keis, H. Lindstrom, S. Sodergren, A. Solbrand, A. Hagfeldt, S. E. Lindquist, and M. Muhammed, *J. Phys. Chem. B.*, 101 (1997) 2598.
55. E. A. Meulenkamp, *J. Phys. Chem. B.*, 103 (1999) 7831.
56. A. Hagfeldt and M. Grätzel, *Chem. Rev.*, 95 (1995) 49.
57. D. I. Suh, S. Y. Lee, T. H. Kim, J. M. Chun, E. K. Suh, O. B. Yang, and S. K. Lee, *Chem. Phys. Lett.*, 442 (2007) 348.

58. L. T. Canham, *Appl. Phys. Lett.*, 57 (1990) 1046.
59. J. J. Kelly and D. Vanmaekelbergh, in G.Hodes (Ed.), *Electrochemistry of Nanomaterials*, WILEY-VCH, Weinheim, 2001, Ch. 4.
60. J. J. Kelly and D. Vanmaekelbergh, *Electrochim. Acta*, 43 (1998) 2773.
61. V. L. Colvin, A. N. Goldstein, and A. P. Alivisatos, *J. Am. Chem. Soc.*, 114 (1992) 5221.
62. M. Miyake, H. Matsumoto, M. Nishizawa, T. Sakata, H. Mori, S. Kuwabata, and H. Yoneyama, *Langmuir*, 13 (1997) 742.
63. T. Nakanishi, B. Ohtani, and K. Uosaki, *J. Phys. Chem. B.*, 102 (1998) 1571.
64. K. Hu, M. Brust, and A. J. Bard, *Chem. Mater.*, 10 (1998) 1160.
65. S. Drouard, S. G. Hickey, and J. D. Riley, *Chem. Commun.*, 1 (1999) 67.
66. S. Ogawa, F. F. Ran, and A. J. Bard, *J. Phys. Chem. B*, 99 (1995) 11182.
67. S. Ogawa, K. Hu, F. R. F. Fan, and A. J. Bard, *J. Phys. Chem. B.*, 101 (1997) 5707.
68. D. Chen, G. Wang, W. Lu, H. Zhang, and J. Li, *Electrochem. Commun.*, 9 (2007) 2151.
69. A. Henglein, *Top. Curr. Chem.*, 143 (1988) 115.
70. H. Weller, *Adv. Mater.*, 5 (1993) 88.
71. A. P. Alivisatos, *J. Phys. Chem.*, 100 (1996) 13226.
72. A. N. Shipway, E. Katz, and I. Willner, *Chem. Phys. Chem.*, 1 (2000) 18.
73. B. Alperson, H. Demange, I. Rubinstein, and G. Hodes, *J. Phys. Chem. B.*, 103 (1999) 4943.
74. G. Hodes, T. Engelhard, A. Albuayron, and A. Pettford Long, *Mat. Res. Soc. Symp.*, (1990).
75. D. Gal, G. Hodes, D. Hariskos, D. Braunger, and H. W. Schock, *Appl. Phys. Lett.*, 73 (1998) 3135.
76. H. Jia, Y. Hu, Y. Tang, and L. Zhang, *Electrochem. Commun.*, 8 (2006) 1381.
77. S. Licht, G. Hodes, R. Tenne, and J. Manassen, *Nature*, 326 (1987) 863.
78. S. Licht, B. Wang, T. Soga, and M. Umeno, *Appl. Phys. Lett.*, 74 (1999) 4055.
79. M. Sharon, P. Veluchamy, C. Natrajan, and C. D. Kumar, *Electrochim. Acta*, 36 (1991) 1107.
80. B. Wang, S. Licht, and M. Umeno, *Sol. Energy Mater. Sol. Cells*, 64 (2000) 311.
81. A. J. Bard and L. R. Faulkner, *Electrochemical Methods: Fundamentals and Applications*, John Wiley & Sons, Inc. New York, 2001.
82. F. E. Beideman and D. M. Hercules, *J. Phys. Chem.*, 83 (1979) 2203.
83. R. Y. Lai and A. J. Bard, *J. Phys. Chem. A.*, 107 (2003) 3335.
84. X. B. Yin, S. Dong, and E. wang, *Trends Anal. Chem.*, 23 (2004) 432.
85. I. Rubinstein and A. J. Bard, *J. Am. Chem. Soc.*, 103 (1981) 512.
86. H. D. Abruna and A. J. Bard, *J. Am. Chem. Soc.*, 104 (1982) 2641.
87. D. Ege, W. G. Becker, and A. J. Bard, *Anal. Chem.*, 56 (1984) 2413.
88. J. K. Leland and M. J. Powell, *J. Electrochem. Soc.*, 137 (1990) 3127.
89. J. B. Noffsinger and N. D. Danielson, *Anal. Chem.*, 59 (1987) 865.
90. M. M. Collinson and R. M. Wightman, *Anal. Chem.*, 65 (1993) 2576.
91. W. Miao, in C.G.Zoski (Ed.), *Handbook of Electrochemistry*, Elsevier, Amsterdam, 2007, Ch. 13.
92. Y. Greenwald, F. Hide, J. Gao, F. Wudl, and A. J. Heeger, *J. Electrochem. Soc.*, 144 (1997) L70.
93. Q. Pei, G. Yu, C. Zhang, Y. Yang, and A. J. Heeger, *Science*, 269 (1995) 1086.
94. D. Dini, *Chem. Mater.*, 17 (2005) 1933.
95. J. Gao, A. J. Heeger, I. H. Campbell, and D. L. Smith, *Phys. Rev. B*, 59 (1999) R2482.
96. R. H. Friend, R. W. Gymer, A. B. Holmes, J. H. Burroughes, R. N. Marks, C. Taliani, D. D. C. Bradley, D. A. Dos Santos, J. L. Bredas, M. Logdlund, and W. R. Salaneck, *Nature*, 397 (1999) 121.
97. Y. Hu, Y. Zhang, and J. Gao, *Adv. Mater.*, 18 (2006) 2880.
98. C. Tracy and J. Gao, *J. Appl. Phys.*, 100 (2006) 104503.
99. Y. Zhang and J. Gao, *J. Appl. Phys.*, 100 (2006) 084501.

100. J. Gao and J. Dane, *Appl. Phys. Lett.*, 84 (2004) 2778.
101. J. Gao and J. Dane, *J. Appl. Phys.*, 98 (2005) 063513.
102. J. Gao and J. Dane, *Appl. Phys. Lett.*, 83 (2003) 3027.
103. J. H. Shin, N. D. Robinson, S. Xiao, and L. Edman, *Advanced Functional Materials*, 17 (2007) 1807.
104. Y. G. Zhang, Y. F. Hu, and J. Gao, *Appl. Phys. Lett.*, 88 (2006) 163507.
105. D. T. Simon, D. B. Stanislowski, and S. A. Carter, *Applied Physics Letters*, 90 (2007) 103508.
106. J. Gao, G. Yu, and A. J. Heeger, *Appl. Phys. Lett.*, 71 (1997) 1293.
107. J. Dane, C. Tracy, and J. Gao, *Appl. Phys. Lett.*, 86 (2005) 153509.
108. Y. Zhang, Y. Hu, and J. Gao, *Appl. Phys. Lett.*, 88 (2006) 163507.
109. C. Tracy and J. Gao, *Appl. Phys. Lett.*, 87 (2005) 143502.
110. Y. Shao, G. C. Bazan, and A. J. Heeger, *Advanced Materials*, 19 (2007) 365.
111. A. A. Argun, P. H. Aubert, B. C. Thompson, I. Schwendeman, C. L. Gaupp, J. Hwang, N. J. Pinto, D. B. Tanner, A. G. MacDiarmid, and J. R. Reynolds, *Chem. Mater.*, 16 (2004) 4401.
112. T. Tatsuma and K. Suzuki, *Electrochem. Commun.*, 9 (2007) 574.